

UC Davis

UC Davis Previously Published Works

Title

Epoxyeicosatrienoic acid (EET)-stimulated angiogenesis is mediated by epoxy hydroxyeicosatrienoic acids (EHETs) formed from COX-2

Permalink

<https://escholarship.org/uc/item/1955p9m1>

Journal

Journal of Lipid Research, 60(12)

ISSN

0022-2275

Authors

Rand, Amy A
Rajamani, Anita
Kodani, Sean D
[et al.](#)

Publication Date

2019-12-01

DOI

10.1194/jlr.m094219

Peer reviewed



Epoxyeicosatrienoic acid (EET)-stimulated angiogenesis is mediated by epoxy hydroxyeicosatrienoic acids (EHETs) formed from COX-2^S

Amy A. Rand,^{*,†,§} Anita Rajamani,^{**} Sean D. Kodani,^{†,§} Todd R. Harris,^{*,†,§} Lukas Schlatt,^{†,§} Bodgan Barnych,^{†,§} Anthony G. Passerini,^{**} and Bruce D. Hammock^{1,†,§}

Department of Chemistry,^{*} Carleton University, Ottawa, ON, Canada; and Department of Entomology and Nematology,[†] Department of Biomedical Engineering,^{**} and UC Davis Comprehensive Cancer Center,[§] University of California, Davis, Davis, CA

Abstract Epoxyeicosatrienoic acids (EETs) are formed from the metabolism of arachidonic acid by cytochrome P450s. EETs promote angiogenesis linked to tumor growth in various cancer models that is attenuated in vivo by cyclooxygenase 2 (COX-2) inhibitors. This study further defines a role for COX-2 in mediating endothelial EET metabolism promoting angiogenesis. Using human aortic endothelial cells (HAECs), we quantified 8,9-EET-induced tube formation and cell migration as indicators of angiogenic potential in the presence and absence of a COX-2 inducer [phorbol 12,13-dibutyrate (PDBu)]. The angiogenic response to 8,9-EET in the presence of PDBu was 3-fold that elicited by 8,9-EET stabilized with a soluble epoxide hydrolase inhibitor (*t*-TUCB). Contributing to this response was the COX-2 metabolite of 8,9-EET, the 11-hydroxy-8,9-EET (8,9,11-EHET), which exogenously enhanced angiogenic responses in HAECs at levels comparable to those elicited by vascular endothelial growth factor (VEGF). In contrast, the 15-hydroxy-8,9-EET isomer was also formed but inactive. The 8,9,11-EHET also promoted expression of the VEGF family of tyrosine kinase receptors. These results indicate that 8,9-EET-stimulated angiogenesis is enhanced by COX-2 metabolism in the endothelium through the formation of 8,9,11-EHET. **■** This alternative pathway for the metabolism of 8,9-EET may be particularly important in regulating angiogenesis under circumstances in which COX-2 is induced, such as in cancer tumor growth and inflammation.—Rand, A. A., A. Rajamani, S. D. Kodani, T. R. Harris, L. Schlatt, B. Barnych, A. G. Passerini, and B. D. Hammock. Epoxyeicosatrienoic acid (EET)-stimulated angiogenesis is mediated by epoxy hydroxyeicosatrienoic acids (EHETs) formed from COX-2. *J. Lipid Res.* 2019. 60: 1996–2005.

Supplementary key words arachidonic acid • endothelial cells • cyclooxygenase 2 • mass spectrometry • cancer • metabolism • soluble epoxide hydrolase • angiogenesis

Epoxyeicosatrienoic acids (EETs) are biologically active omega-6 fatty acids generated through the cytochrome P450 (CYP) oxidation of arachidonic acid (ARA). Endothelial cells express endogenous levels of CYP2B, CYP2C, and CYP2J subfamilies, which form four EET regioisomers (5,6-EET, 8,9-EET, 11,12-EET, and 14,15-EET) (1, 2). EETs can also be formed by other CYPs, particularly when they are induced (3). The EETs act in part to change the membrane potential and tone of the vascular wall; they are strong vasodilators that lead to reduced blood pressure (4, 5) and are endothelium-derived hyperpolarizing factors that activate Ca²⁺-activated K⁺ channels in vascular smooth muscle cells and coronary arteries (6, 7). EETs also act as secondary messengers in numerous signal-transduction pathways involved in inflammation (8), pain (9), bone growth (10), cell migration (11), apoptosis (12), platelet aggregation (13), and hypoxia/reoxygenation injury (14). Multiple studies have also demonstrated that EETs stimulate endothelial cell proliferation and angiogenesis (1, 15–23).

Angiogenesis is a tightly regulated physiological process that provides oxygen during tissue repair and growth but is also central to the growth and spread of tumors. EETs,

Abbreviations: ARA, arachidonic acid; COX, cyclooxygenase; CYP, cytochrome P450; DHET, dihydroxyeicosatrienoic acid; EET, epoxyeicosatrienoic acid; EHET, epoxy hydroxyeicosatrienoic acid; HAEC, human aortic endothelial cell; PDBu, phorbol 12,13-dibutyrate; sEH, soluble epoxide hydrolase; *t*-AUCB, *trans*-4-(4-(3-adamantan-1-yl-ureido)-cyclohexyloxy)-benzoic acid; THET, trihydroxyeicosatrienoic acid; *t*-TUCB, *trans*-4-[4-(3-trifluoromethoxyphenyl-ureido)-cyclohexyloxy]benzoic acid; VEGF, vascular endothelial growth factor; VEGFR, VEGF receptor.

¹To whom correspondence should be addressed.

e-mail: bdhammock@ucdavis.edu

■ The online version of this article (available at <http://www.jlr.org>) contains a supplement.

This work was supported by National Institutes of Health Grants ROI ES0027010, P42 ES004699, R35 ES030443 (B.D.H.), T32 CA108459 (A.A.R.), and R01 HL082689 (A.G.P.); the 2016 American Association for Cancer Research Judah Folkman Fellowship for Angiogenesis Research (A.A.R.); and Natural Sciences and Engineering Research Council of Canada Grant RGPIN-2018-05330. The content is solely the responsibility of the authors and does not necessarily represent the official views of the National Institutes of Health.

Manuscript received 26 March 2019 and in revised form 27 September 2019.

Published, *JLR Papers in Press*, October 22, 2019

DOI <https://doi.org/10.1194/jlr.M094219>

Copyright © 2019 Rand et al. Published under exclusive license by The American Society for Biochemistry and Molecular Biology, Inc.

This article is available online at <http://www.jlr.org>

when exogenously administered, have been shown to induce endothelial cell proliferation and angiogenesis in various *in vitro* and *in vivo* models (24–29). The mechanism for this activity is associated with protein activation within the PI3K/Akt and MAPK signal-transduction cascades (1, 17, 19, 21, 22) and increased expression of angiogenic growth factors, including vascular endothelial growth factor (VEGF) (18), fibroblast growth factor 2 (17), and epidermal growth factor (23). In cancer models, EET-induced angiogenesis supports the growth and metastasis of tumors. Overexpressing CYP2J2 in endothelial cells leads to increased primary tumor growth and metastasis in multiple tumor models that is dependent, at least in part, on EET induction of VEGF (30).

The biological activity of EETs can be short-lived because they are rapidly metabolized by soluble epoxide hydrolase (sEH), which hydrates the epoxide group to form diols [dihydroxyeicosatrienoic acids (DHETs)] that are inactive in the context of angiogenesis. sEH inhibitors such as *trans*-4-(4-(3-adamantan-1-yl-ureido)-cyclohexoxyl)-benzoic acid (*t*-AUCB) stabilize levels of EETs *in vivo*, prolonging their biological activity, and are currently in development to treat various diseases (31, 32). An enigma is that when sEH inhibitors, which increase levels of angiogenic EETs, are used in combination with chemotherapeutic agents (e.g., COX-2 inhibitors and cisplatin) in models of angiogenesis and tumorigenesis, there is a dramatically antiangiogenic response and reduction in tumor growth and metastasis (33–37). While EETs activate several distinct angiogenic signaling cascades, recent evidence has shown that EET angiogenic activity may be further dependent upon downstream metabolites formed from cyclooxygenase (COX) (38). COX-2 inhibitors directly affect EET-dependent tumor growth (33). While *t*-AUCB at high doses was shown to increase cancer tumor growth due to stabilized levels of EETs, the combination of the COX-2 inhibitor celecoxib with *t*-AUCB reduced angiogenesis and tumorigenesis below the levels achieved with a COX-2 inhibitor alone in three mouse models of cancer (33, 34, 37). Synthesis of a compound that simultaneously inhibits both COX-2 and sEH (PTUPB) was also more effective at inhibiting primary tumor growth and metastasis than inhibitors selective to either pathway (33, 35). The evidence that EET-dependent angiogenic and tumorigenic activity is modified by the combined treatment of COX-2 and sEH inhibitors suggests that there is crosstalk between these pathways, the nature of which has not been completely described.

While EET hydroxylation by sEH has been thoroughly examined, EET hydroxylation by COX has received much less attention. This has been partly due to the assumption that the presence of an epoxide on the 8,9-, 11,12-, and 14,15-positions of ARA would prevent the usual endoperoxide formation and limit reactivity. We were the first to examine the reactivity of the four EET regioisomers with purified COX-1 and COX-2 (38, 39). The 5,6-EET forms prostaglandin (5,6-epoxy-PGE₁ and hydroxyl-PGI₁) (38, 40–42), thromboxane (5-hydroxy-6,9-epoxy-thromboxane B₁), and hydroxylated (5,6-epoxy-12-hydroxyheptadecadienoic acid) products (43). 8,9-EET and 11,12-EET are both

capable of being metabolized by COX-1 and COX-2 but form only hydroxylated products (38, 39). The hydroxylation of 8,9-EET has also been demonstrated in human platelets and ram seminal vesicles (44).

We and others have shown that EETs are metabolized by COX-1 and COX-2 to produce prostaglandin-like analogues and epoxy hydroxyeicosatrienoic acids (EHETs) (38, 40, 41, 44, 45). Using synthesized EHETs, we previously demonstrated that 8,9,11-EHET increased cell infiltration and microvessel formation in an *in vivo* Matrigel assay, while its regioisomer, 8,9,15-EHET, was inactive (38). Here, our objective was to further define the relative roles of COX-2 and sEH in regulating EET metabolism by endothelium as it relates to angiogenesis. We hypothesized that COX-2 induction would shift EET metabolism toward the production of EHETs, which function to promote angiogenesis. We show that the enhanced angiogenesis elicited by 8,9-EET within human aortic endothelial cells (HAECs) is further increased upon COX-2 induction due to the formation of 8,9,11-EHET, which specifically acts to promote endothelial cell migration and tube formation through a VEGF receptor (VEGFR)-dependent mechanism (Fig. 1).

MATERIALS AND METHODS

Materials

HAEC cell media supplemented with a SingleQuots EGM bullet kit was obtained from Lonza (Allendale, NJ). Eicosanoid standards were obtained from Cayman Chemical (Ann Arbor, MI) except for the following synthesized in house: 8,9,11-EHET and 8,9,15-EHET methyl esters (39), 8,9-EET (46), and 8,9,11-trihydroxyeicosatrienoic acid (THET) and 8,9,15-THET (38). All lipid substrates were dissolved in ethanol to form stock solutions (10–100 mM) and stored under nitrogen at –20°C until use. Phorbol

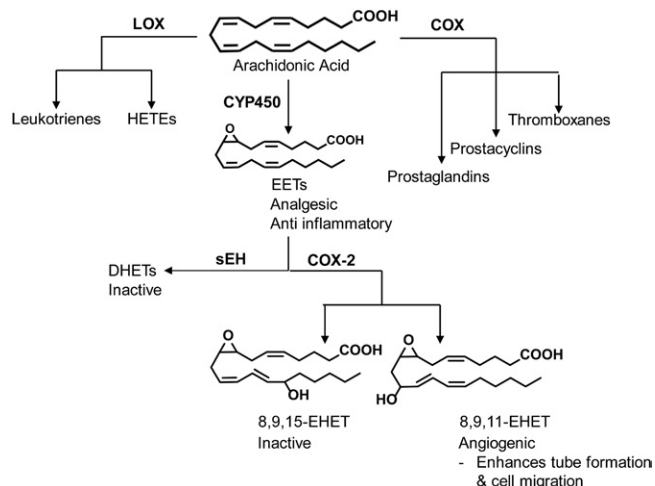


Fig. 1. ARA is metabolized by COX, LOX (lipoxygenase), and CYP to form bioactive oxylipins. The CYP pathway produces EETs that are analgesic and anti-inflammatory. When COX-2 is expressed in HAECs, EETs can undergo further metabolism to yield the angiogenic 8,9,11-EHET. The effect is more potent when combined with sEH inhibition, which prevents the conversion of EETs to inactive DHETs.

12,13-dibutyrate (PDBu) was purchased from Sigma-Aldrich (St. Louis, MO). For LC/MS/MS analysis, the EHET and THET methyl esters were cleaved to acids using carboxyl esterase 2 enzyme hydrolysis as previously described (38). The sEH inhibitor *trans*-4-[4-(3-trifluoromethoxyphenyl-l-ureido)-cyclohexyloxy] benzoic acid (*t*-TUCB) was also synthesized in house (47). This sEH inhibitor was used because it has a similar structure and potency to *t*-AUCB but is more metabolically stable (48). Water was either 18 mQ or LC/MS grade (Thermo Fisher Scientific, Waltham, MA). Ultima LC/MS grade methanol and acetonitrile were purchased from Sigma-Aldrich.

HAEC growth and maintenance

HAEC passages 6–8 (lot #2228 derived from a 21-year-old female and lot #7F4409 from a 34-year-old male; Genlantis, San Diego, CA) were cultured in EGM-2 (Lonza) supplemented with 1× antibiotic/antimycotic (Thermo Fisher Scientific). Cells were seeded on 6-, 12-, or 24-well tissue culture plates (Falcon; Thermo Fisher Scientific) and proliferated to form an 85% to 95% confluent monolayer.

Lipid extraction and LC/MS/MS analysis

The protocol is detailed in the supplemental data. In brief, oxylipin metabolites were extracted from HAEC culture medium and cell lysates using solid-phase extraction and quantified by UPLC/MS/MS. Extracted oxylipins were separated using a Phenomenex Kinetex C18 column (15 × 2.1 mm, 1.7 μm, 100 Å; Torrance, CA), with LC/MS-grade water and acetonitrile (both containing 0.1% acetic acid) as mobile phases for the gradient UPLC method. All analytes were monitored in multiple reaction monitoring mode as parent and product ion mass transition pairs. Oxylipins were identified and quantified based on LC retention time and their multiple reaction monitoring transitions.

Synthesis of EHETs by HAECs

To study whether EHETs and their corresponding sEH products, the THETs, could be formed enzymatically by HAECs, cells at passage 7 were seeded onto 6-well plates and grown to confluence. The cells were serum-starved for 3 h, and the COX-2 inducer PDBu and/or sEH inhibitor *t*-TUCB ($C_f = 1 \mu\text{M}$) were added in DMSO after 2 h of serum starvation, followed by 8,9-EET in ethanol ($C_f = 1 \mu\text{M}$). FBS was added to a final concentration of 2%. After 20 h, the media were removed from the plates, and the cells were lysed on ice with ice-cold methanol and nonpyrogenic cell scrapers. Samples were stored at -20°C before extraction and LC/MS/MS analysis.

Tube formation assay

Capillary tube formation was analyzed using the Ibidi μ-slide angiogenesis plates. This assay was chosen as our primary in vitro model for angiogenesis because it encompasses the major steps of sprouting, proliferation, and migration and facilitates endothelial cell reassembling and new cell-cell contacts necessary for tube formation. The 15-well μ-slide plates were coated with 10 μl growth factor-reduced Matrigel and incubated for 30 min at 37°C . Endothelial cells were first serum- and VEGF-starved for 3 h before passaging. The cells (1×10^4) were plated over the solidified Matrigel (10 μl) in 50 μl serum-free media with 8,9-EET or EHETs in ethanol (0.001–1 μM). To determine the effect of 8,9-EET on tube formation with and without COX-2 induction and sEH inhibition, HAECs were plated on Matrigel in 50 μl serum-starved media, and 8,9-EET was added in ethanol to a final concentration of 0.1 μM in the presence of *t*-TUCB ($C_f = 1 \mu\text{M}$) and/or PDBu ($C_f = 1 \mu\text{M}$). All lipid treatments were also paired with vehicle (ethanol) controls. After 24 h, cells were stained with Calcein AM. Media were

removed by gentle aspiration and replaced with 50 μl serum-free media containing 6.25 μg/ml Calcein AM. The plates were incubated in the dark for 30 min at room temperature. Tube structures were recorded by taking a fluorescence image of the entire well at 485 nm/529 nm. To quantify the tube network formation, total tube length was measured either manually with the analyzer blinded to the treatment description or by using Fiji software (49). Experiments were performed at least in triplicate.

Migration assay

The migration rate of HAECs was analyzed using a scratch-wound technique. HAECs were seeded in 24-well tissue culture plates, maintained at 37°C and 5% CO_2 , and grown to 90% to 95% confluent monolayers. HAECs were FBS- and VEGF-starved for 3 h before adding lipid treatments in ethanol (0.001–1 μM) in 500 μl serum- and VEGF-free media. A 200 μl pipette tip was used to scratch the endothelial monolayer and produce a wound. Cell migration was monitored every 2 h at the exact coordinates over a period of 24 h using a Nikon Eclipse TE2000-U microscope at 10× and quantified using Fiji. All treatments were performed in triplicate.

Western blot analysis

To evaluate the sEH, COX-1, and COX-2 expression levels, HAECs (3×10^5) were plated on 6-well plates with full media supplemented with an EGM SingleQuots bullet kit with and without 8,9-EET (1 μM) for 24 h. The cells were lysed with 200 μl RIPA buffer (Thermo Fisher Scientific) with a protease inhibitor cocktail (Sigma-Aldrich). Lysate protein was prepared by dilution in 4× LDS Sample Buffer and 10× Reducing Buffer (Thermo Fisher Scientific). Protein was loaded on Bolt 4–12% Bis-Tris gels (Thermo Fisher Scientific) and then electrophoresed for 35 min at 200 V. Protein was then transferred to 0.45 μm pore-sized nitrocellulose membranes using the Pierce FastBlotter (Thermo Fisher Scientific). The blot was blocked with 3% BSA in TBST and incubated with either primary rabbit polyclonal anti-human sEH antibody (1:5000), rabbit monoclonal anti-human COX-2 antibody (1:1000) (#12282, Cell Signaling Technology, Danvers, MA), or rabbit monoclonal anti-human COX-1 antibody (1:1000) (#9896, Cell Signaling Technology). Blots were subsequently incubated with secondary goat anti-rabbit IgG (1:5000) conjugated with HRP (Abcam, Cambridge, MA). Bands were detected using the SuperSignal West Femto ECL Detection Reagent (Thermo Fisher Scientific) and visualized with the ChemiDoc MP (Bio-Rad Laboratories, Hercules, CA). Band intensity was quantified using ImageLab 5.0 (Bio-Rad Laboratories). Purified COX-1, COX-2, and sEH were used as positive controls. Each treatment was analyzed in triplicate.

Human angiogenesis antibody array

Confluent HAEC monolayers were FBS- and VEGF-starved for 3 h. A scratch wound was created using a 200 μl pipette tip, and cells were treated with ethanol (vehicle control; $n = 3$), 8,9-EET (0.1 μM; $n = 3$), or 8,9,11-EHET (0.01 μM; $n = 3$). Culture media were collected and pooled for the RayBio C Series human angiogenesis antibody array (C1000). The assay was conducted as instructed with pooled nondiluted culture samples. The array was imaged using the Western blot ChemiDoc MP imaging system (Bio-Rad Laboratories) until the positive control had strong comparable signal among all arrays. Measurements of integrated signal density ($n = 1–2$) were acquired using the Fiji plugin microarray profile. A square region of interest with an identical area was used to measure the integrated signal density across all images. These measurements were compiled, the percentages were normalized with respect to the control, and the data were plotted in SigmaPlot 14.0 (Systat Software, Inc., San Jose, CA) to qualitatively

observe the difference in angiogenic profiles. Although the expression of the VEGFR family members 2 and 3 each was increased, they were combined to make the statistical analysis possible.

Statistical analyses

Data are reported as arithmetic means \pm SEs. Statistical comparisons between groups were made by one-way ANOVA followed by the Holm-Sidak pairwise or control comparison, as described in each figure caption. Differences were considered significant for two-tailed $P < 0.05$. All statistical calculations were performed using SigmaPlot 14.0.

RESULTS

8,9-EET-stimulated angiogenesis is enhanced by COX-2

While all EET regioisomers have been shown to be mildly angiogenic, 8,9-EET was the focus for this study because it was the best substrate for COX-1 and COX-2, having the lowest measured K_M and a high k_{cat} (38). To understand whether 8,9-EET-stimulated angiogenesis can be modified by COX-2, we dosed HAECs with 8,9-EET in the presence and absence of a synthetic phorbol ester COX-2 inducer, PDBu, and monitored the amount of tube formation over a period of 24 h (Fig. 2A). Given that PDBu

induces COX-2, we also monitored levels of the endogenous prostaglandin E₂, the angiogenic oxylipin formed from COX metabolism of ARA (Fig. 2B). While PDBu triggers many other tumor-promoting pathways, it was used for two reasons: to test the hypothesis that COX-2 metabolizes the 8,9-EET to products that enhance angiogenesis and to compare its angiogenic capacity as a known tumor promoter to the sEH inhibitor *t*-TUCB. 8,9-EET (0.1 μ M) doubled tube formation compared with the vehicle (ethanol) control group (Fig. 2), consistent with results from previous studies (1, 50). The addition of *t*-TUCB did not significantly increase tube formation beyond that elicited by 8,9-EET alone. Inducing COX-2 with PDBu (1 μ M) further enhanced tube formation in the presence or absence of 8,9-EET, resulting in values that were 7-fold that of the vehicle control. COX-2 induction also formed PGE₂ at detectable levels for all treatment groups. These levels were not dependent on 8,9-EET treatment, given that 8,9-EET treated and untreated cells produced PGE₂ at similar levels. Combining *t*-TUCB with PDBu brought the angiogenic response back to vehicle control levels in the absence of 8,9-EET. In contrast, the presence of 8,9-EET with *t*-TUCB and PDBu markedly increased angiogenic tube formation, doubling the response over treatment with 8,9-EET alone.

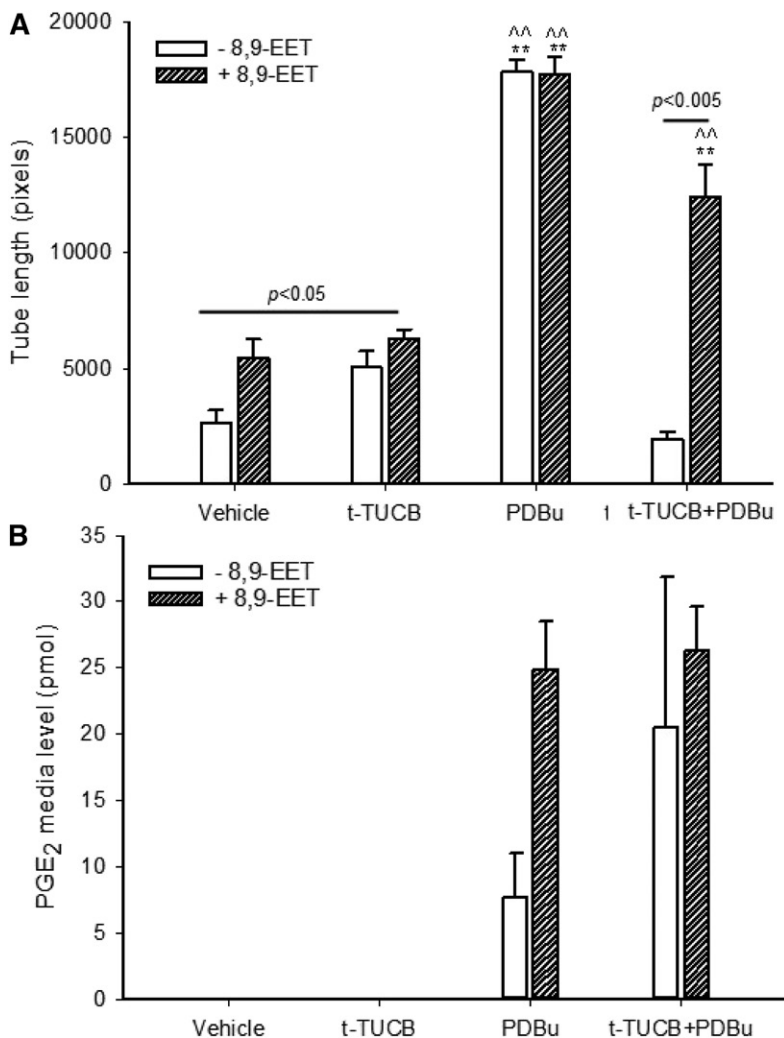


Fig. 2. COX-2 induction, partly driven by PGE₂, enhances tube formation. A: HAECs in basal media (in the absence of serum and VEGF) were seeded onto 15-well μ -angiogenesis plates with growth factor-reduced Matrigel. Cells were then treated with vehicle or 8,9-EET (0.1 μ M) in the presence and absence of the sEH inhibitor *t*-TUCB (1 μ M), COX-2 inducer PDBu (1 μ M), or *t*-TUCB and PDBu combined. Tube length was measured manually using Fiji. Values are means \pm SEs ($n = 4$). B: HAEC cells (300,000) were incubated with and without 8,9-EET (0.1 μ M) with full media (3 ml) with and without the sEH inhibitor *t*-TUCB and COX-2 inducer PDBu for 20 h. PGE₂ levels (pmol) in media were analyzed using LC/MS/MS. Values are means \pm SEs ($n = 2-3$). ** $P < 0.001$ versus the vehicle control with and without 8,9-EET; ^^ $P < 0.001$ versus the *t*-TUCB treatment with and without the 8,9-EET. Statistical tests were performed using one-way ANOVA with Holm-Sidak pairwise analysis. The raw data used for this figure are reported in supplemental Table S1.

While PGE₂ is a known angiogenic factor contributing to some of these COX-2-driven responses, to further explain these results we investigated 8,9-EET metabolites downstream of COX-2 for their angiogenic potential.

COX-2 metabolizes 8,9-EET to form 8,9,11-EHET and 8,9,15-EHET in HAECs

We and others have shown that two regioisomers form from the metabolism of 8,9-EET by COX, 8,9,11-EHET and 8,9,15-EHET (38, 39, 44), but the formation of these metabolites has not been demonstrated in endothelial cells. To investigate this, we dosed HAECs with 8,9-EET (1 μM) with and without *t*-TUCB and PDBu and incubated the cells for 20 h. The media and cell lysates were collected, extracted, and analyzed for 8,9-EET and its sEH and COX products using LC/MS/MS. Endogenous levels of these lipids were also examined by treating cells with *t*-TUCB and/or PDBu in the absence of 8,9-EET, but metabolite levels were all below the limit of detection (not shown). For HAECs treated with 8,9-EET, DHET and/or EHET metabolites were primarily observed in the media (Fig. 3). Only a small percentage (approximately 2%) of total metabolite production was detected in the cell lysates, at levels two orders of magnitude lower than in the media (supplemental Fig. S1). Treatment with 8,9-EET resulted in similar detectable levels of 8,9-DHET compared with all other treatments. Inducing COX-2 resulted in significant production of both 8,9,11-EHET and 8,9,15-EHET, observed in the cell media. Levels of 8,9,11-EHET were about twice those of the

8,9-DHET formed by the same treatments. The production of 8,9,11-EHET was 6-fold higher than 8,9,15-EHET. Trace levels of 8,9,11-THET and 8,9,15-THET, the sEH hydrolysis products of 8,9,11-EHET and 8,9,15-EHET, were also detected.

Intracellular levels of sEH, COX-1, and COX-2 protein were measured by Western blot in the presence and absence of 8,9-EET (Fig. 4, supplemental Fig. S2). All protein responses were normalized with respect to β-actin. For all treatments, sEH/β-actin ratios were comparatively no different from COX-1/β-actin ratios. The sEH/β-actin and COX-1/β-actin ratios were also not significantly different between vehicle, *t*-TUCB, and *t*-TUCB + PDBu treatments, suggesting that the sEH inhibitor and COX-2 inducer had no effect on sEH or COX-1 protein expression. In contrast, PDBu treatment yielded significantly higher COX-2 levels compared with treatments without PDBu in accordance with previous studies (Fig. 4) (51). The COX-2/β-actin ratio after COX-2 induction was also about 2-fold higher than sEH expression. Together these results demonstrate that COX-2 induction in endothelial cells leads to enhanced metabolism of 8,9-EET to form EHETs over DHETs.

8,9,11-EHET promotes HAEC tube formation

In our previous study, we identified 8,9,11-EHET but not 8,9,15-EHET to be angiogenic in an in vivo mouse Matrigel model (38). Here, we investigated the roles that these COX metabolites of 8,9-EET have on the angiogenic processes of tube formation and cell migration. We measured tube formation using fluorescence microscopy in response to lipid treatments after 24 h, comparing the 8,9,11-EHET and

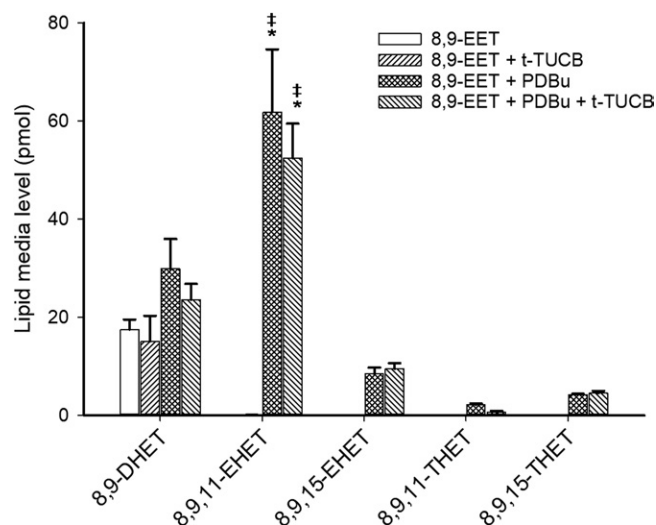


Fig. 3. 8,9 EET is metabolized by sEH to form 8,9-DHET and COX-2 to form 8,9,11-EHET and 8,9,15-EHET, which are further metabolized to THETs. 8,9-EET (1 μM) was incubated with HAEC cells (300,000) with full media (3 ml) with and without the sEH inhibitor *t*-TUCB and COX-2 inducer PDBu for 20 h. Levels of lipids (pmol) from the media were analyzed using LC/MS/MS. Values are averages from one to four independent experiments, each having three to four replicates. Error bars are means ± SEs. **P* < 0.05 versus the 8,9-DHET formed from PDBu treatment with and without *t*-TUCB; †*P* < 0.05 versus the 8,9,15-EHET formed from PDBu treatment with and without *t*-TUCB. Statistical tests were performed using one-way ANOVA with Holm-Sidak pairwise analysis. The raw data used for this figure are reported in supplemental Table S2.

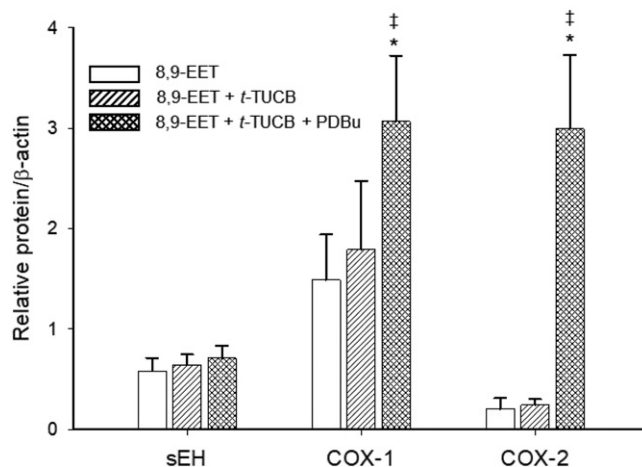


Fig. 4. COX-1 and sEH are expressed in basal HAECs, and COX-2 expression is induced by PDBu. Western blot analysis of sEH, COX-1, and COX-2 in HAEC cell extracts. 8,9-EET (1 μM) was incubated with HAEC cells (300,000) with full media (3 ml) with and without the sEH inhibitor *t*-TUCB and COX-2 inducer PDBu for 24 h. The graph shows quantification of Western blot bands, where protein responses were normalized with respect to β-actin. Equal amounts of protein from the vehicle and treatment groups were analyzed in triplicate. **P* < 0.05 versus the COX-2 expression in the vehicle and *t*-TUCB groups; †*P* < 0.05 versus sEH expression (all treatments). Statistical tests were performed using one-way ANOVA with Holm-Sidak pairwise analysis. The raw data used for this figure is reported in supplemental Table S3.

8,9,15-EHET over a range of concentrations (0.001–1 μM) (Fig. 5A). The 8,9,11-EHET was active at all concentrations, with the maximum effect occurring at 0.01 μM , a 3-fold increase from the vehicle control. At this concentration, 8,9,11-EHET produced similar action to the VEGF positive control ($P = 0.1$). In contrast to 8,9,11-EHET, the 8,9,15-EHET was not potent in mediating tube formation, in that it yielded a response no different than the vehicle control over the tested concentration range. An MTT assay was used to test whether EHET treatments were influencing cell survival; EHET incubation had no noticeable effect on cell number over 24 h (supplemental Fig. S3). In comparison to the tumor promoter and COX-2 inducer PDBu, 8,9,11-EHET was much less potent at mediating tube formation. Treatment with PDBu (1 μM) produced a robust angiogenic response, 3-fold higher than the responses for 8,9,11-EHET and 8,9-EET (Table 1).

8,9,11-EHET enhances HAEC migration

We used the scratch assay to examine the influence of 8,9,11-EHET and 8,9,15-EHET on HAEC migration rate, quantified by first calculating the cell-surface coverage within the initial cell-free gap over 24 h and the rate at which HAECs filled the scratch gap (cell-front velocity) after the addition of oxylipins (Fig. 6). VEGF (2 ng/ml), full media, and PGE₂ were used as positive controls for comparison. In general, 8,9,11-EHET treatments promoted HAEC migration 2- to 3-fold over the vehicle control, indicating that 8,9,11-EHET could enhance wound repair. In contrast, 8,9,15-EHET had no effect on the migration rate across all tested concentrations. Together these data establish 8,9,11-EHET, but not 8,9,15-EHET, as a potent mediator of endothelial proangiogenic activity.

8,9,11-EHET increases expression of soluble VEGFR

To determine the role of angiogenic signaling factors in 8,9,11-EHET-induced angiogenesis, we studied the response of several human angiogenic factors secreted during tube formation using an angiogenesis array. Both 8,9-EET and 8,9,11-EHET treatment significantly increased the expression of secreted VEGFR-2 and VEGFR-3 (Fig. 7). Compared with the control, treatment with 8,9-EET or 8,9,11-EHET increased the expression of these receptors about 3-fold. In contrast, other factors measured in the

array had no significant effect on 8,9,11-EHET-induced tube formation, suggesting most of the 8,9,11-EHET angiogenic activity arises from the VEGF tyrosine kinase receptor-dependent pathways. These data also demonstrate that 8,9,11-EHET alone elicits angiogenic signaling in the absence of other more powerful promoters such as PDBu. The raw data for Fig. 7, as well as those factors tested but not significantly different, are shown in supplemental Table S6.

DISCUSSION

Major findings of this study in HAEC are consistent with previous reports on the angiogenic activity of EETs and their stabilization by sEH inhibitors in vivo. The data support our hypothesis that COX-2 induction shifts EET metabolism toward the production of EHETs over DHETs, which contributes to their angiogenic activity. Specifically, we report for the first time that 1) EHETs are produced by endothelial cells under conditions in which COX-2 is induced, 2) the angiogenic activity of 8,9-EET is in part mediated by the COX-2 metabolite 8,9,11-EHET, 3) migration and tube formation are stimulated by direct incubation with the COX metabolite 8,9,11-EHET but not the 8,9,15-EHET isomer, 4) 8,9-EET is normally metabolized by HAECs predominantly by sEH to the corresponding diol 8,9-DHET, 5) induction of COX-2 by PDBu shifts 8,9-EET metabolism toward the proangiogenic 8,9,11-EHET at a level twice that of 8,9-DHET, 6) HAEC migration stimulated by 8,9,11-EHET is dependent on the overexpression of the VEGFRs, and 7) although the increase in 8,9-EET and 8,9,11-EHET induced tube formation is statistically significant in some cases, the increase is trivial compared with that elicited by the phorbol ester PDBu, a well-known tumor-promoting agent that increases COX-2 and PGE₂. Together these results suggest that much if not all of the angiogenic effect of 8,9-EET is due to its metabolism by COX-2. These data at least partially explain why combining an sEH and COX-2 inhibitor or an integrated dual inhibitor blocks angiogenesis, tumor growth, and metastasis in some murine cancer models (31–34).

Many studies have shown that COX-2 and CYP metabolites of ARA stimulate angiogenesis in endothelial cells (52, 53). However, much less is known about crosstalk between

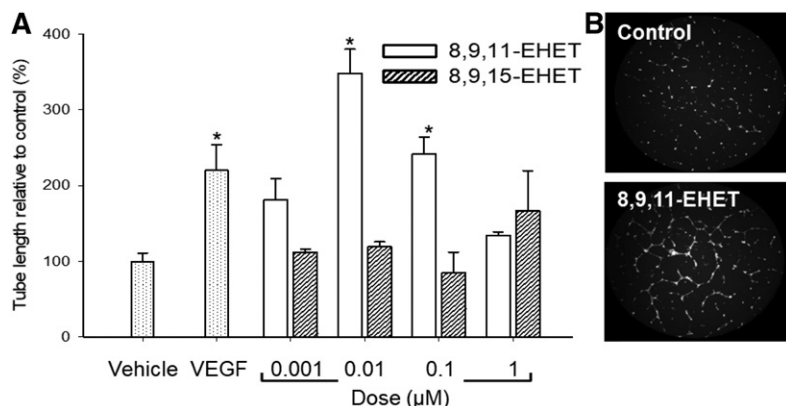


Fig. 5. 8,9,11-EHET enhances HAEC tube formation. A: HAECs in basal media were seeded onto a 15-well μ -angiogenesis plate with growth factor-reduced Matrigel. Cells were treated with vehicle, VEGF (2 ng/ml), or various concentrations of 8,9,11-EHET or 8,9,15-EHET for 24 h. Tube formation was observed using a fluorescence microscope after staining with Calcein. Tube length was measured using Fiji. B: Representative images of HAEC tube formation after a 24 h incubation with vehicle and the 8,9,11-EHET treatment (0.1 μM). Values are means \pm SEs ($n = 3$). * $P < 0.05$ versus the control. Statistical tests were performed using one-way ANOVA with Holm-Sidak comparison to the control analysis. The raw data used for this figure are reported in supplemental Table S4.

TABLE 1. PDBu induces HAEC tube formation more than 8,9-EET and 8,9,11-EHET treatments

Treatment	Tube Length vs. Control (%)	Sample size (n)
Vehicle	100 ± 11	12
VEGF	220 ± 34*	5
8,9-EET	209 ± 31	4
8,9,11-EHET	242 ± 23*	3
8,9,15-EHET	85 ± 28	3
<i>t</i> -TUCB	194 ± 27	4
PDBu	681 ± 30*	4

HAECs in basal media (in the absence of serum and VEGF) were seeded onto a 15-well μ -angiogenesis plates with growth factor-reduced Matrigel. Cells were then treated with vehicle (ethanol) or separately incubated with 8,9-EET (0.1 μ M), 8,9,11-EHET (0.1 μ M), or PDBu (1 μ M). Tube length was measured manually using Fiji. The analysis was blinded toward treatments to avoid bias. Values are means \pm SEs ($n = 3-12$). * $P < 0.05$ versus the control. Statistical tests were performed using one-way ANOVA with Holm-Sidak comparison to the control analysis.

these branches. In HUVECs, CYP2C9 overexpression stimulated greater endogenous EET production, which surprisingly also increased COX-2 expression (54). Similarly, exogenous addition of 11,12-EET also increased COX-2 expression, indicating another mechanism of crosstalk between the COX and CYP pathways (54). This treatment enhanced tube formation through the increased production of PGE₂ as well as the proangiogenic prostacyclin and PGI₂ (20, 55, 56). While we did not find that 8,9-EET affected COX-2 expression (Fig. 4) or contribute to increased PGE₂ (Fig. 2B), the angiogenic response from 8,9-EET was enhanced in the presence of PDBu, indicating crosstalk between the CYP and COX-2 pathways. PDBu is a powerful tumor promoter that participates in several signaling

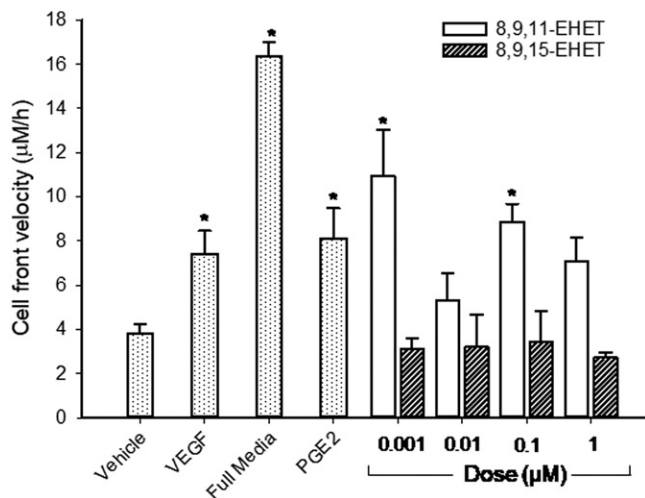


Fig. 6. 8,9,11-EHET enhances HAEC migration. HAECs in basal media (in the absence of serum and VEGF) were seeded onto a 24-well plate, serum-starved for 3 h, and treated with vehicle (ethanol), growth factors (VEGF and full media), PGE₂ (1 μ M), and varying concentrations of EHETs. Cell-surface coverage over 24 h was captured using a brightfield microscope and quantified using Fiji. Values are means \pm SEs ($n = 3-6$). * $P < 0.05$ versus the vehicle control. Statistical tests were performed using one-way ANOVA with Holm-Sidak comparison to the control analysis. The raw data used for this figure are reported in supplemental Table S5.

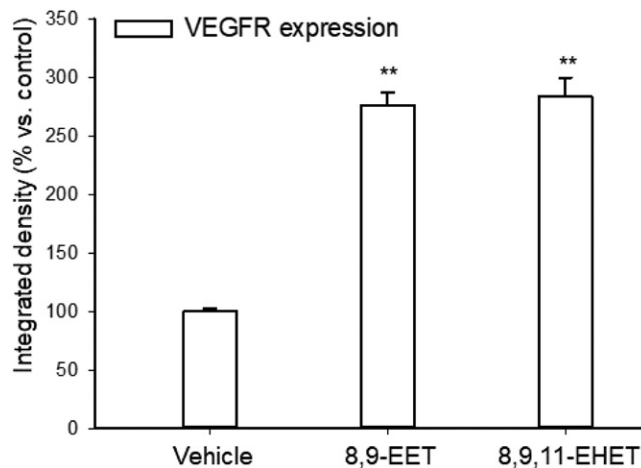


Fig. 7. 8,9-EET and 8,9,11-EHET increase VEGFR expression. HAECs were FBS- and VEGF-starved for 3 h. Cells were scratched with a pipette tip and treated with 0.01 μ M 8,9,11-EHET, 0.1 μ M 8,9-EET, or ethanol (vehicle). The VEGFR-2 and -3 expression in culture media was imaged, and integrated signal density was calculated using Fiji. Values are means \pm SEs ($n = 2-4$). ** $P < 0.001$ versus the vehicle control. Statistical tests were performed using one-way ANOVA with Holm-Sidak pairwise analysis. The raw data used for this figure are reported in supplemental Table S6.

pathways, including the induction of COX-2. In this study, we quantified increased levels of 8,9,11-EHET (from exogenous 8,9-EET) and PGE₂ (from endogenous ARA) after PDBu treatment that contributed to its robust angiogenic response. However, given the participation of PDBu in several signaling pathways, other factors may be controlling the observed angiogenic response and cannot be discounted. Its strong effect on increasing tube length dwarfs the effect of the results from *t*-TUCB, 8,9-EET, 8,9,11-EHET, and 8,9,15-EHET (Fig. 2, Table 1). In this respect, while EETs can be angiogenic, they are weaker agents compared with these other known angiogenic factors. However, our data also suggest that in circumstances with increased COX-2 expression, 8,9-EET becomes a more potent mediator of angiogenesis. This activity is controlled in part by 8,9-EET metabolism to 8,9,11-EHET. COX-2 expression is upregulated along with increased PGE₂ in various tumors and cancer cells (57, 58), its induction acting as a switch to promote angiogenesis in order to provide nutrients for tumor growth. In support of this claim, inhibiting COX-2 reduces the size of induced tumors in mice by blocking angiogenic mediators (33, 59, 60), which may include the 8,9,11-EHET.

As presented in Fig. 2A, the sEH inhibitor *t*-TUCB decreased tube formation after COX-2 induction only in the absence of 8,9-EET. This was surprising because *t*-TUCB should stabilize endogenous EET levels, leading to enhanced tube formation, as observed when we incubated *t*-TUCB with 8,9-EET without COX-2 induction. However, endogenous EETs were not observed within any treatment; all levels were below the LC/MS/MS limit of detection. This may explain why treatment with *t*-TUCB alone had little effect on tube formation. In conditions in which EET levels are low, adding an sEH inhibitor in combination with

highly angiogenic factors (e.g., PDBu) may suppress angiogenesis. The antiproliferative action of an sEH inhibitor has previously been shown in HUVECs (33). Additional studies will be required to elucidate the mechanism by which sEH inhibitors influence angiogenesis in both the presence and absence of EETs.

We have previously demonstrated that 8,9-EET converts to 8,9,11-EHET using purified ovine COX-1 and human recombinant COX-2 enzymes (38, 39). It was therefore surprising that 8,9-EET produced 8,9-DHET as its sole metabolite, irrespective of the presence of COX-1. This suggests that either the basal enzyme expression of sEH is higher than COX-1 or that 8,9-EET has a higher turnover (k_{cat}/K_M) for sEH versus COX-1. Western blot data showed no significant difference between COX-1/ β -actin ratios and sEH/ β -actin ratios, indicating similar sEH and COX-1 expression levels. Therefore, 8,9-EET may have a higher kinetic turnover for sEH than COX-1. Further study is warranted, as COX-1 kinetics with 8,9-EET has only been established in its purified ovine form (38). The induction of COX-2 yielded both 8,9,11-EHET and 8,9,15-EHET metabolites and their sEH-produced THET metabolites at levels significantly higher than 8,9 DHET from the same treatments. Western blot revealed that the increased relative COX-2 expression levels exceeded those of sEH, giving rise to increased production of the EHETs. In addition, an examination of the k_{cat}/K_M values for 8,9-EET metabolism by sEH and COX-2 reveals approximately 24-fold greater turnover by COX-2 (38), suggesting that the bioavailability of EHETs is greater than the sEH products when COX-2 is induced. This implies that increased COX-2 expression shifts EET metabolism from sEH-driven DHET formation to COX-2-driven EHET formation. Once formed, the 8,9,11-EHET can undergo hydrolysis by sEH. However, compared with 8,9-EET hydrolysis, the K_M and k_{cat} values for 8,9,11-EHET hydrolysis are lower (38). Thus, based on enzyme kinetics and hydrolysis being the rate-limiting reaction, while the EHETs have greater chemical polarity, they have similar stability to epoxide hydration as 8,9-EET and are able to exert their biological action.

The 8,9,11-EHET is a renal vasoconstrictor and a potent glomerular mitogen, at least an order of magnitude more potent than the 8,9-EET (45). Our previous study demonstrated that the 8,9,11-EHET was angiogenic using a Matrigel in vivo mouse model, whereas the 8,9,15-EHET was inactive (38). Both tube formation and migration, two major angiogenic markers, were enhanced upon exposure to 8,9,11-EHET and gave similar responses to the angiogenic growth factor VEGF (Table 1, Fig. 5). The lipids had no effect on cell survival, suggesting that the relative variation in their angiogenic response was independent of their effect on apoptosis (supplemental Fig. S3). While 8,9,11-EHET has not yet been observed in vivo, it may form at similar levels to the EETs (between 0.75 and 300 nM in endothelial cells) under circumstances in which COX-2 is induced (61). The added concentration of 8,9,11-EHET ranged from 0.001 to 1 μ M and, in general, promoted tube formation and migration across this concentration range. Additional studies will be necessary to establish the potency

of 8,9,11-EHET relative to important angiogenic eicosanoids, such as the COX-derived prostaglandins. In contrast, 8,9,15-EHET did not show any appreciable activity in this model. It is currently unknown whether this oxylipin participates in other biologically important pathways.

Endothelial cell migration and tube formation are critical events in angiogenesis. Many studies have demonstrated a role for VEGFR-2 and VEGFR-3 in mediating angiogenesis due to their high affinity for the proangiogenic VEGF-A or VEGF-C and VEGF-D, respectively (62). The EETs elicit endothelial cell proliferation and angiogenesis, and many signaling pathways have been implicated over the past decade (25, 26, 29, 53). For instance, signaling molecules modulated by EETs include VEGF, mitogen-activated protein kinases, phosphatidylinositol 3-kinase, protein kinase A, COX-2, and several transcription factors (63, 64). In the current study, the expression of VEGFR-2 and VEGFR-3 was enhanced by 8,9,11-EHET. This response mimics that of previous findings for 8,9-EET, which was dependent in part on the VEGF-dependent PI3K/Akt pathway to stimulate migration and tube formation (1). These results explain, at least in part, the enigma surrounding EET angiogenic signaling in the presence and absence of COX-2 inhibitors; although EETs and sEH inhibitors are mildly angiogenic, treatment with a COX-2 inhibitor dramatically reverses the response to one that is potently antiangiogenic. The same antiangiogenic response is observed with the dual sEH and COX-2 inhibitor PTUPB, which acts in synergy with the chemotherapeutic agent cisplatin (36, 37). In addition, because the omega-3 fatty acids EPA and DHA are poor substrates for COX-2 and the omega or terminal olefin of omega-3 fatty acids are by far the best substrate for CYP catalyzed epoxidation rather than an internal olefin (65), this argument also may explain why sEH inhibitors, when given with an omega-3-enriched diet, reduce angiogenesis, tumor growth, and metastasis (66).

In conclusion, we demonstrate for the first time that 8,9-EET metabolism is shifted toward the production of the proangiogenic 8,9,11-EHET in endothelial cells upon the induction of COX-2 and that this oxylipin may be mediating its proangiogenic activity through the VEGFR-2/3 signaling pathway. These findings reveal crosstalk between the pathways that regulate EET metabolism, with important ramifications for understanding angiogenesis in the context of tumor growth. Notably, these results may help explain how sEH inhibitors when used with celecoxib, or inhibitors that jointly target COX and sEH, not only are antiangiogenic but also in fact block tumor growth and metastasis (33, 34). ■

REFERENCES

1. Pozzi, A., I. Macias-Perez, T. Abair, S. Wey, Y. Su, R. Zent, J. R. Falck, and J. H. Capdevila. 2005. Characterization of 5, 6-and 8, 9-epoxyeicosatrienoic acids (5, 6-and 8, 9-EET) as potent in vivo angiogenic lipids. *J. Biol. Chem.* **280**: 27138–27146.
2. Zeldin, D. C. 2001. Epoxygenase pathways of arachidonic acid metabolism. *J. Biol. Chem.* **276**: 36059–36062.
3. Lee, C. A., B. P. Lawrence, N. I. Kerkvliet, and A. B. Rifkind. 1998. 2,3,7,8-Tetrachlorodibenzo-p-dioxin induction of cytochrome

- P450-dependent arachidonic acid metabolism in mouse liver microsomes: evidence for species-specific differences in responses. *Toxicol. Appl. Pharmacol.* **153**: 1–11.
4. Sinal, C. J., M. Miyata, M. Tohkin, K. Nagata, J. R. Bend, and F. J. Gonzalez. 2000. Targeted disruption of soluble epoxide hydrolase reveals a role in blood pressure regulation. *J. Biol. Chem.* **275**: 40504–40510.
 5. Yu, Z., F. Xu, L. M. Huse, C. Morisseau, A. J. Draper, J. W. Newman, C. Parker, L. Graham, M. M. Engler, B. D. Hammock, et al. 2000. Soluble epoxide hydrolase regulates hydrolysis of vasoactive epoxyeicosatrienoic acids. *Circ. Res.* **87**: 992–998.
 6. Campbell, W. B., P. F. Pratt, and D. R. Harder. 1996. Identification of epoxyeicosatrienoic acids as endothelium-derived hyperpolarizing factors. *Circ. Res.* **78**: 415–423.
 7. Fisslthaler, B., R. Popp, L. Kiss, M. Potente, D. R. Harder, I. Fleming, and R. Busse. 1999. Cytochrome P450 2C is an EDHF synthase in coronary arteries. *Nature*. **401**: 493–497.
 8. Node, K., Y. Huo, X. Ruan, B. Yang, M. Spiecker, K. Ley, D. C. Zeldin, and J. K. Liao. 1999. Anti-inflammatory properties of cytochrome P450 epoxygenase-derived eicosanoids. *Science*. **285**: 1276–1279.
 9. Wagner, K. M., C. B. McReynolds, W. K. Schmidt, and B. D. Hammock. 2017. Soluble epoxide hydrolase as a therapeutic target for pain, inflammatory and neurodegenerative diseases. *Pharmacol. Ther.* **180**: 62–76.
 10. Trindade-da-Silva, C. A., A. Bettaieb, M. H. Napimoga, K. S. S. Lee, B. Inceoglu, C. Ueira-Vieira, D. Bruun, S. K. Goswami, F. G. Haj, and B. D. Hammock. 2017. Soluble epoxide hydrolase pharmacological inhibition decreases alveolar bone loss by modulating host inflammatory response, RANK-related signaling, endoplasmic reticulum stress, and apoptosis. *J. Pharmacol. Exp. Ther.* **361**: 408–416.
 11. Sun, J., X. Sui, J. A. Bradbury, D. C. Zeldin, M. S. Conte, and J. K. Liao. 2002. Inhibition of vascular smooth muscle cell migration by cytochrome p450 epoxygenase-derived eicosanoids. *Circ. Res.* **90**: 1020–1027.
 12. Chen, J-K., J. Capdevila, and R. C. Harris. 2001. Cytochrome p450 epoxygenase metabolism of arachidonic acid inhibits apoptosis. *Mol. Cell. Biol.* **21**: 6322–6331.
 13. Krötz, F., T. Riexinger, M. A. Buerkle, K. Nithipatikom, T. Gloe, H. Y. Sohn, W. B. Campbell, and U. Pohl. 2004. Membrane potential-dependent inhibition of platelet adhesion to endothelial cells by epoxyeicosatrienoic acids. *Arterioscler. Thromb. Vasc. Biol.* **24**: 595–600.
 14. Yang, B., L. Graham, M. Dikalov, R. P. Mason, J. R. Falck, J. K. Liao, and D. C. Zeldin. 2001. Overexpression of cytochrome P450 CYP2J2 protects against hypoxia-reoxygenation injury in cultured bovine aortic endothelial cells. *Mol. Pharmacol.* **60**: 310–320.
 15. Zhang, C., and Harder, D. R. 2002. Cerebral capillary endothelial cell mitogenesis and morphogenesis induced by astrocytic epoxyeicosatrienoic acid. *Stroke*. **33**: 2957–2964.
 16. Medhara, M., J. Daniels, K. Munday, B. Fisslthaler, R. Busse, E. R. Jacobs, and Harder, D. R. 2003. Epoxygenase-driven angiogenesis in human lung microvascular endothelial cells. *Am. J. Physiol. Heart Circ. Physiol.* **284**: H215–H224.
 17. Zhang, B., H. Cao, and G. N. Rao. 2006. Fibroblast growth factor-2 is a downstream mediator of phosphatidylinositol 3-kinase-Akt signaling in 14,15-epoxyeicosatrienoic acid-induced angiogenesis. *J. Biol. Chem.* **281**: 905–914.
 18. Cheranov, S. Y., M. Karpurapu, D. Wang, B. Zhang, R. C. Venema, and G. N. Rao. 2008. An essential role for SRC-activated STAT-3 in 14,15-EET-induced VEGF expression and angiogenesis. *Blood*. **111**: 5581–5591.
 19. Yan, G., S. Chen, B. You, and J. Sun. 2008. Activation of sphingosine kinase-1 mediates induction of endothelial cell proliferation and angiogenesis by epoxyeicosatrienoic acids. *Cardiovasc. Res.* **78**: 308–314.
 20. Michaelis, U. R., B. Fisslthaler, E. Barbosa-Sicard, J. R. Falck, I. Fleming, and R. Busse. 2005. Cytochrome P450 epoxygenases 2C8 and 2C9 are implicated in hypoxia-induced endothelial cell migration and angiogenesis. *J. Cell Sci.* **118**: 5489–5498.
 21. Ma, J., L. Zhang, W. Han, T. Shen, C. Ma, Y. Liu, X. Nie, M. Liu, Y. Ran, and D. Zhu. 2012. Activation of JNK/c-Jun is required for the proliferation, survival, and angiogenesis induced by EET in pulmonary artery endothelial cells. *J. Lipid Res.* **53**: 1093–1105.
 22. Wang, Y., X. Wei, X. Xiao, R. Hui, J. W. Card, M. A. Carey, D. W. Wang, and D. C. Zeldin. 2005. Arachidonic acid epoxygenase metabolites stimulate endothelial cell growth and angiogenesis via mitogen-activated protein kinase and phosphatidylinositol 3-kinase/Akt signaling pathways. *J. Pharmacol. Exp. Ther.* **314**: 522–532.
 23. Michaelis, U. R., B. Fisslthaler, M. Medhara, D. Harder, I. Fleming, and R. Busse. 2003. Cytochrome P450 2C9-derived epoxyeicosatrienoic acids induce angiogenesis via cross-talk with the epidermal growth factor receptor (EGFR). *FASEB J.* **17**: 770–772.
 24. Imig, J. D. 2012. Epoxides and soluble epoxide hydrolase in cardiovascular physiology. *Physiol. Rev.* **92**: 101–130.
 25. Fleming, I. 2007. Epoxyeicosatrienoic acids, cell signaling and angiogenesis. *Prostaglandins Other Lipid Mediat.* **82**: 60–67.
 26. Fleming, I. 2011. The cytochrome P450 pathway in angiogenesis and endothelial cell biology. *Cancer Metastasis Rev.* **30**: 541–555.
 27. Panigrahy, D., E. R. Greene, A. Pozzi, D. W. Wang, and D. C. Zeldin. 2011. EET signaling in cancer. *Cancer Metastasis Rev.* **30**: 525–540.
 28. Spector, A. A. 2009. Arachidonic acid cytochrome P450 epoxygenase pathway. *J. Lipid Res.* **50** (Suppl.): S52–S56.
 29. Askari, A., S. J. Thomson, M. L. Edin, D. C. Zeldin, and D. Bishop-Bailey. 2013. Roles of the epoxygenase CYP2J2 in the endothelium. *Prostaglandins Other Lipid Mediat.* **107**: 56–63.
 30. Panigrahy, D., B. T. Kalish, S. Huang, D. R. Bielenberg, H. D. Le, J. Yang, M. L. Edin, C. R. Lee, O. Benny, D. K. Mudge, et al. 2013. Epoxyeicosanoids promote organ and tissue regeneration. *Proc. Natl. Acad. Sci. USA*. **110**: 13528–13533.
 31. Morisseau, C., and B. D. Hammock. 2013. Impact of soluble epoxide hydrolase and epoxyeicosanoids on human health. *Annu. Rev. Pharmacol. Toxicol.* **53**: 37–58.
 32. Newman, J. W., C. Morisseau, and B. D. Hammock. 2005. Epoxide hydrolases: their roles and interactions with lipid metabolism. *Prog. Lipid Res.* **44**: 1–51.
 33. Zhang, G., D. Panigrahy, S. H. Hwang, J. Yang, L. M. Mahakian, H. I. Wettersten, J. Y. Liu, Y. Wang, E. S. Ingham, S. Tam, et al. 2014. Dual inhibition of cyclooxygenase-2 and soluble epoxide hydrolase synergistically suppresses primary tumor growth and metastasis. *Proc. Natl. Acad. Sci. USA*. **111**: 11127–11132.
 34. Li, J., C. Tang, L. Li, R. Li, and Y. Fan. 2016. Quercetin sensitizes glioblastoma to t-AUCB by dual inhibition of Hsp27 and COX-2 in vitro and in vivo. *J. Exp. Clin. Cancer Res.* **35**: 61.
 35. Li, J., Y. Zhou, H. Wang, Y. Gao, L. Li, S. H. Hwang, X. Ji, and B. D. Hammock. 2017. COX-2/sEH dual inhibitor PTUPB suppresses glioblastoma growth by targeting epidermal growth factor receptor and hyaluronan mediated motility receptor. *Oncotarget*. **8**: 87353–87363.
 36. Wang, F., H. Zhang, A-H. Ma, W. Yu, M. Zimmermann, J. Yang, S. H. Hwang, D. Zhu, T. Y. Lin, M. Malfatti, et al. 2018. COX-2/sEH dual inhibitor PTUPB potentiates the anti-tumor efficacy of cisplatin. *Mol. Cancer Ther.* **17**: 474–483.
 37. Gartung, A., J. Yang, V. P. Sukhatme, D. R. Bielenberg, D. Fernandes, J. Chang, B. A. Schmidt, S. H. Hwang, D. Zurakowski, S. Huang, et al. 2019. Suppression of chemotherapy-induced cytokine/lipid mediator surge and ovarian cancer by a dual COX-2/sEH inhibitor. *Proc. Natl. Acad. Sci. USA*. **116**: 1698–1703.
 38. Rand, A. A., B. Barnych, C. Morisseau, T. Cajka, K. S. S. Lee, D. Panigrahy, and B. D. Hammock. 2017. Cyclooxygenase-derived proangiogenic metabolites of epoxyeicosatrienoic acids. *Proc. Natl. Acad. Sci. USA*. **114**: 4370–4375.
 39. Barnych, B., A. A. Rand, T. Cajka, K. S. S. Lee, and B. D. Hammock. 2017. Synthesis of cyclooxygenase metabolites of 8,9-epoxyeicosatrienoic acid (EET): 11- and 15-hydroxy 8,9-EETs. *Org. Biomol. Chem.* **15**: 4308–4313.
 40. Moreland, K. T., J. D. Procknow, R. S. Sprague, J. L. Iverson, A. J. Lonigro, and A. H. Stephenson. 2007. Cyclooxygenase (COX)-1 and COX-2 participate in 5,6-epoxyeicosatrienoic acid-induced contraction of rabbit intralobar pulmonary arteries. *J. Pharmacol. Exp. Ther.* **321**: 446–454.
 41. Carroll, M. A., M. Balazy, P. Margiotta, J. R. Falck, and J. C. McGiff. 1993. Renal vasodilator activity of 5,6-epoxyeicosatrienoic acid depends upon conversion by cyclooxygenase and release of prostaglandins. *J. Biol. Chem.* **268**: 12260–12266.
 42. Oliw, E. H., and G. Benthin. 1985. On the metabolism of epoxyeicosatrienoic acids by ram seminal vesicles: isolation of 5(6) epoxy-prostaglandin F1 α . *Biochem. Biophys. Res. Commun.* **126**: 1090–1096.
 43. Balazy, M. 1991. Metabolism of 5,6-epoxyeicosatrienoic acid by the human platelet. Formation of novel thromboxane analogs. *J. Biol. Chem.* **266**: 23561–23567.
 44. Zhang, J. Y., C. Prakash, K. Yamashita, and I. A. Blair. 1992. Regiospecific and enantioselective metabolism of 8,9-epoxyeicosatrienoic acid by cyclooxygenase. *Biochem. Biophys. Res. Commun.* **183**: 138–143.

45. Homma, T., J. Y. Zhang, T. Shimizu, C. Prakash, I. A. Blair, and R. C. Harris. 1993. Cyclooxygenase-derived metabolites of 8,9-epoxyeicosatrienoic acid are potent mitogens for cultured rat glomerular mesangial cells. *Biochem. Biophys. Res. Commun.* **191**: 282–288.
46. Falck, J. R., P. Yadagiri, and J. Capdevila. 1990. Synthesis of epoxyeicosatrienoic acids and heteroatom analogs. In *Methods in Enzymology*. R. C. Murphy and F. A. Fitzpatrick, editors. Academic Press, San Diego, CA. 357–364.
47. Hwang, S. H., H.-J. Tsai, J.-Y. Liu, C. Morisseau, and B. D. Hammock. 2007. Orally bioavailable potent soluble epoxide hydrolase inhibitors. *J. Med. Chem.* **50**: 3825–3840.
48. Liu, J.-Y., Y.-P. Lin, H. Qiu, C. Morisseau, T. E. Rose, S. H. Hwang, N. Chiamvimonvat, and B. D. Hammock. 2013. Substituted phenyl groups improve the pharmacokinetic profile and anti-inflammatory effect of urea-based soluble epoxide hydrolase inhibitors in murine models. *Eur. J. Pharm. Sci.* **48**: 619–627.
49. Schindelin, J., I. Arganda-Carreras, E. Frise, V. Kaynig, M. Longair, T. Pietzsch, S. Preibisch, C. Rueden, S. Saalfeld, B. Schmid, et al. 2012. Fiji: an open-source platform for biological-image analysis. *Nat. Methods.* **9**: 676–682.
50. Zhang, C., and D. R. Harder. 2002. Cerebral capillary endothelial cell mitogenesis and morphogenesis induced by astrocytic epoxyeicosatrienoic acid. *Stroke.* **33**: 2957–2964.
51. Morita, I. 2002. Distinct functions of COX-1 and COX-2. *Prostaglandins Other Lipid Mediat.* **68–69**: 165–175.
52. Rüegg, C., O. Dormond, and A. Mariotti. 2004. Endothelial cell integrins and COX-2: mediators and therapeutic targets of tumor angiogenesis. *Biochim. Biophys. Acta.* **1654**: 51–67.
53. Imig, J. D. 2016. Epoxyeicosatrienoic acids and 20-hydroxyeicosatetraenoic acid on endothelial and vascular function. *Adv. Pharmacol.* **77**: 105–141.
54. Michaelis, U. R., J. R. Falck, R. Schmidt, R. Busse, and I. Fleming. 2005. P450^{2C9}-derived epoxyeicosatrienoic acids induce the expression of cyclooxygenase-2 in endothelial cells. *Arterioscler. Thromb. Vasc. Biol.* **25**: 321–326.
55. Wang, D., and R. N. DuBois. 2010. Eicosanoids and cancer. *Nat. Rev. Cancer.* **10**: 181–193.
56. Salcedo, R., X. Zhang, H. A. Young, N. Michael, K. Wasserman, W.-H. Ma, M. Martins-Green, W. J. Murphy, and J. J. Oppenheim. 2003. Angiogenic effects of prostaglandin E2 are mediated by up-regulation of CXCR4 on human microvascular endothelial cells. *Blood.* **102**: 1966–1977.
57. Hugo, H. J., C. Saunders, R. G. Ramsay, and E. W. Thompson. 2015. New insights on COX-2 in chronic inflammation driving breast cancer growth and metastasis. *J. Mammary Gland Biol. Neoplasia.* **20**: 109–119.
58. Eibl, G., D. Bruemmer, Y. Okada, J. P. Duffy, R. E. Law, H. A. Reber, and O. J. Hines. 2003. PGE₂ is generated by specific COX-2 activity and increases VEGF production in COX-2-expressing human pancreatic cancer cells. *Biochem. Biophys. Res. Commun.* **306**: 887–897.
59. Saukkonen, K., J. Rintahaka, A. Sivula, C. J. Buskens, B. P. Van Rees, M.-C. Rio, C. Haglund, J. J. Van Lanschot, G. J. Offerhaus, and A. Ristimäki. 2003. Cyclooxygenase-2 and gastric carcinogenesis. *APMIS.* **111**: 915–925.
60. Xu, L., J. Stevens, M. B. Hilton, S. Seaman, T. P. Conrads, T. D. Veenstra, D. Logsdon, H. Morris, D. A. Swing, N. L. Patel, et al. 2014. COX-2 inhibition potentiates antiangiogenic cancer therapy and prevents metastasis in preclinical models. *Sci. Transl. Med.* **6**: 242ra84.
61. Dhanasekaran, A., R. Al-Saghir, B. Lopez, D. Zhu, D. D. Gutterman, E. R. Jacobs, and M. Medhara. 2006. Protective effects of epoxyeicosatrienoic acids on human endothelial cells from the pulmonary and coronary vasculature. *Am. J. Physiol. Heart Circ. Physiol.* **291**: H517–H531.
62. Shibuya, M. 2013. Vascular endothelial growth factor and its receptor system: physiological functions in angiogenesis and pathological roles in various diseases. *J. Biochem.* **153**: 13–19.
63. Michaelis, U. R., and I. Fleming. 2006. From endothelium-derived hyperpolarizing factor (EDHF) to angiogenesis: epoxyeicosatrienoic acids (EETs) and cell signaling. *Pharmacol. Ther.* **111**: 584–595.
64. Panigrahy, D., A. Kaipainen, E. R. Greene, and S. Huang. 2010. Cytochrome P450-derived eicosanoids: the neglected pathway in cancer. *Cancer Metastasis Rev.* **29**: 723–735.
65. Arnold, C., M. Markovic, K. Blossey, G. Wallukat, R. Fischer, R. Dechend, A. Konkel, C. von Schacky, F. C. Luft, D. N. Müller, et al. 2010. Arachidonic acid-metabolizing cytochrome P450 enzymes are targets of ω -3 fatty acids. *J. Biol. Chem.* **285**: 32720–32733.
66. Zhang, G., D. Panigrahy, L. M. Mahakian, J. Yang, J.-Y. Liu, K. S. S. Lee, H. I. Wettersten, A. Ulu, X. Hu, S. Tam, et al. 2013. Epoxy metabolites of docosahexaenoic acid (DHA) inhibit angiogenesis, tumor growth, and metastasis. *Proc. Natl. Acad. Sci. USA.* **110**: 6530–6535.